



The role of phase coherence in seeded supercontinuum generation

Sørensen, Simon Toft; Larsen, Casper; Møller, Uffe; Moselund, M.; Thomsen, Carsten L.; Bang, Ole

Published in:
Optics Express

Link to article, DOI:
[10.1364/OE.20.022886](https://doi.org/10.1364/OE.20.022886)

Publication date:
2012

Document Version
Publisher's PDF, also known as Version of record

[Link back to DTU Orbit](#)

Citation (APA):
Sørensen, S. T., Larsen, C., Møller, U., Moselund, M., Thomsen, C. L., & Bang, O. (2012). The role of phase coherence in seeded supercontinuum generation. *Optics Express*, 20(20), 22886-22894. <https://doi.org/10.1364/OE.20.022886>

General rights

Copyright and moral rights for the publications made accessible in the public portal are retained by the authors and/or other copyright owners and it is a condition of accessing publications that users recognise and abide by the legal requirements associated with these rights.

- Users may download and print one copy of any publication from the public portal for the purpose of private study or research.
- You may not further distribute the material or use it for any profit-making activity or commercial gain
- You may freely distribute the URL identifying the publication in the public portal

If you believe that this document breaches copyright please contact us providing details, and we will remove access to the work immediately and investigate your claim.

The role of phase coherence in seeded supercontinuum generation

Simon Toft Sørensen,^{1,*} Casper Larsen,¹ Uffe Møller,¹
Peter M. Moselund,² Carsten L. Thomsen,² and Ole Bang^{1,2}

¹*DTU Fotonik, Department of Photonics Engineering, Technical University of Denmark, 2800 Kgs. Lyngby, Denmark*

²*NKT Photonics A/S, Blokken 84, DK-3460, Birkerød, Denmark*

**stso@fotonik.dtu.dk*

Abstract: The noise properties of a supercontinuum can be controlled by modulating the pump with a seed pulse. In this paper, we numerically investigate the influence of seeding with a partially phase coherent weak pulse or continuous wave. We demonstrate that the noise properties of the generated supercontinuum are highly sensitive to the degree of phase noise of the seed and that a nearly coherent seed pulse is needed to achieve a coherent pulse break-up and low noise supercontinuum. The specific maximum allowable linewidth of the seed laser is found to decrease with increasing pump power.

© 2012 Optical Society of America

OCIS codes: (030.1640) Coherence; (190.4370) Nonlinear Optics, fibers; (190.4380) Nonlinear optics, four-wave mixing; (320.6629) Supercontinuum generation.

References and links

1. J. M. Dudley, G. Genty, and S. Coen, "Supercontinuum generation in photonic crystal fiber," *Rev. Mod. Phys.* **78**, 1135–1184 (2006).
2. U. Møller, S. T. Sørensen, C. Jakobsen, J. Johansen, P. M. Moselund, C. L. Thomsen, and O. Bang, "Power dependence of supercontinuum noise in uniform and tapered PCFs," *Opt. Express* **20**, 2851–2857 (2012).
3. D. R. Solli, C. Ropers, and B. Jalali, "Active control of rogue waves for stimulated supercontinuum generation," *Phys. Rev. Lett.* **101**, 233902 (2008).
4. P. M. Moselund, M. H. Frosz, C. L. Thomsen, and O. Bang, "Back-seeding of higher order gain processes in picosecond supercontinuum generation," *Opt. Express* **16**, 11954–11968 (2008).
5. G. Genty, J. Dudley, and B. Eggleton, "Modulation control and spectral shaping of optical fiber supercontinuum generation in the picosecond regime," *Appl. Phys. B* **94**, 187–194 (2009).
6. G. Genty and J. Dudley, "Route to coherent supercontinuum generation in the long pulse regime," *IEEE J. Quantum Electron.* **45**, 1331–1335 (2009).
7. N. Brauckmann, M. Kues, T. Walbaum, P. Groß, and C. Fallnich, "Experimental investigations on nonlinear dynamics in supercontinuum generation with feedback," *Opt. Express* **18**, 7190–7202 (2010).
8. D. R. Solli, B. Jalali, and C. Ropers, "Seeded supercontinuum generation with optical parametric down-conversion," *Phys. Rev. Lett.* **105**, 233902 (2010).
9. K. K. Y. Cheung, C. Zhang, Y. Zhou, K. K. Y. Wong, and K. K. Tsia, "Manipulating supercontinuum generation by minute continuous wave," *Opt. Lett.* **36**, 160–162 (2011).
10. Q. Li, F. Li, K. K. Y. Wong, A. P. T. Lau, K. K. Tsia, and P. K. A. Wai, "Investigating the influence of a weak continuous-wave-trigger on picosecond supercontinuum generation," *Opt. Express* **19**, 13757–13769 (2011).
11. S. T. Sørensen, C. Larsen, U. Møller, P. M. Moselund, C. L. Thomsen, and O. Bang, "Influence of pump power and modulation instability gain spectrum on seeded supercontinuum and rogue wave generation," *J. Opt. Soc. Am. B* **29**, 2875–2885 (2012).
12. J. Laegsgaard, "Mode profile dispersion in the generalised nonlinear Schrödinger equation," *Opt. Express* **15**, 16110–16123 (2007).
13. S. B. Cavalcanti, G. P. Agrawal, and M. Yu, "Noise amplification in dispersive nonlinear media," *Phys. Rev. A* **51**, 4086–4092 (1995).

14. M. H. Frosz, "Validation of input-noise model for simulations of supercontinuum generation and rogue waves," *Opt. Express* **18**, 14778–14787 (2010).
15. J. M. Dudley and S. Coen, "Coherence properties of supercontinuum spectra generated in photonic crystal and tapered optical fibers," *Opt. Lett.* **27**, 1180–1182 (2002).
16. S. T. Sørensen, O. Bang, B. Wetzel, and J. M. Dudley, "Describing supercontinuum noise and rogue wave statistics using higher-order moments," *Opt. Commun.* **285**, 2451 – 2455 (2012).
17. G. Genty, M. Surakka, J. Turunen, and A. T. Friberg, "Complete characterization of supercontinuum coherence," *J. Opt. Soc. Am. B* **28**, 2301–2309 (2011).
18. P. M. Moselund, "Long-pulse supercontinuum light sources," Ph.D. thesis (Technical University of Denmark, 2009).

1. Introduction

The noise properties of supercontinuum (SC) generation have attracted a lot of attention due to a large application demand for low noise SC sources [1, 2]. Commercial SC sources are typically based on high-power picosecond or nanosecond pump lasers. For such lasers the pulse break-up is initiated by noise-driven modulational instability (MI), which causes large shot-to-shot fluctuations. It has been demonstrated that the noise can be significantly reduced by modulating the pump pulse in order to ensure a deterministic rather than noise-driven pulse breakup [3–11]. Seeding was numerically investigated in [5, 6, 10, 11]. In all cases a phase coherent seed was used to achieve a coherent pulse break-up through the amplification of a cascade of four-wave mixing (FWM) side-bands. Experimentally, seeding was investigated in [3, 4, 7–9]. In [3, 8, 9] the seed was used to trigger sub-threshold SC generation. The seed was generated by stretching and filtering a fraction of the pump in [3], while [8] used the signal and idler from an optical parametric amplifier as pump and seed. In [9] a separate continuous wave (CW) source was used as seed. It is thus fair to assume that the seeds in [3, 8, 9] were at least partially coherent with the pump. In [4, 7] the generated SC from one pulse was used as a broadband seed for the following pulse either by back-seeding or using a ring cavity. SC generation with feedback is however dynamically different from the approach used in this work, where the pump pulse is modulated with a seed as in [3, 5, 6, 8–11].

While it has thus been shown that seeding can reduce the SC noise, this has been for coherent seeds. In this paper, we numerically investigate the influence of pump power and the phase coherence of the seed on the seeding process, and demonstrate the need for seeding nearly coherently to get a deterministic pulse break-up and thus an improvement in noise. This has, to the best of our knowledge, not been shown before. The results are important in designing seeded low noise SC sources.

2. Numerical model and statistical analysis

We base the numerical work on solutions to the generalised nonlinear Schrödinger equation (GNLSE), which is known to produce spectra and noise properties in excellent agreement with experiments [1]. The GNLSE includes the effects of nonlinearities, the delayed Raman effect, self-steepening and higher-order dispersion necessary to accurately simulate pulse propagation in nonlinear fibers. We used the particular implementation described in [12] with the GNLSE solved in the interaction picture by an adaptive step-size fourth order Runge-Kutta solver. Noise was included as a background of one photon with a random phase in each discretisation bin. Additionally, noise was added to the seed pulse obtained from a physically justified phase-diffusion model [13, 14]. This model assumes fluctuations of the temporal phase, $\delta\phi(t)$, with zero ensemble mean, which results in a Lorentzian spectrum of linewidth $\Delta\nu_{\text{FWHM}}$. The noise linewidth, $\Delta\nu_{\text{FWHM}}$, is the only free parameter of the phase-diffusion model. Experimentally the noise linewidth will typically be fixed for a given laser source.

For the sake of simplicity, we assume a perfectly phase coherent pump and add phase noise

to the seed only. For a Gaussian pump and seed with the same temporal width, T_0 , and peak powers P_p and P_s , respectively, the input field can thus be written as,

$$A(t) = \sqrt{P_p} \exp \left[\frac{-t^2}{2T_0^2} \right] + \sqrt{P_s} \exp \left[\frac{-t^2}{2T_0^2} \right] e^{i\Omega_{\text{mod}} t} \exp [i\delta\phi(t)] + A_{\text{OPPM}} \quad (1)$$

where Ω_{mod} is the modulation frequency of the seed relative to the pump and A_{OPPM} is the one photon per mode background noise. Both the background noise and the phase noise of the seed were varied from simulation to simulation. It should be noted that in Eq. (1) the Lorentzian power spectrum of the phase-diffusion model is convolved with the Gaussian power spectrum of the seed.

Ensemble statistics were calculated by carrying out simulations under identical conditions apart from the initial noise. The noise of the generated SC is quantified with the phase-sensitive spectral coherence function calculated from independent spectra, $\tilde{A}_i(\omega)$, [15],

$$|g_{12}^{(1)}(\omega)| = \left| \frac{\langle \tilde{A}_i^*(\omega) \tilde{A}_j(\omega) \rangle_{i \neq j}}{\sqrt{\langle |\tilde{A}_i(\omega)|^2 \rangle \langle |\tilde{A}_j(\omega)|^2 \rangle}} \right|, \quad (2)$$

where the angle brackets denote ensemble averages and the asterisk denotes complex conjugation. We will further use the overall coherence, $\int_0^\infty |g_{12}^{(1)}(\omega)| \langle |\tilde{A}(\omega)|^2 \rangle d\omega / \int_0^\infty \langle |\tilde{A}(\omega)|^2 \rangle d\omega$, to get a single value for the degree of coherence of an SC ensemble. The intensity noise is quantified by the signal-to-noise ratio (SNR) defined as the ratio of the mean, $\mu(\omega) = \langle |\tilde{A}_i(\omega)|^2 \rangle$, to the standard deviation, $\sigma(\omega) = (\langle |\tilde{A}_i(\omega)|^2 \rangle^2 - \mu(\omega)^2)^{1/2}$,

$$\text{SNR}(\omega) = \frac{\mu(\omega)}{\sigma(\omega)}. \quad (3)$$

The SNR is inversely proportional to the coefficient of variation introduced as an SC noise measure in [16], and is related to the relative intensity noise (RIN) used in most experiments on laser noise.

In the simulations we used a photonic crystal fiber (PCF) with pitch $\Lambda = 3.6 \mu\text{m}$ and hole-to-pitch ratio $d/\Lambda = 0.52$, which gives a zero-dispersion wavelength of 1054 nm. The dispersion, effective area and MI gain spectrum are shown in Fig. 1. We used a Gaussian pump at 1064 nm with a peak power of $P_p = 250 \text{ W}$ and temporal width $T_{\text{FWHM}} = 3 \text{ ps}$. The seed had the same temporal width but only 5% of the peak power, and was given a frequency offset of 3 THz relative to the pump, i.e. a wavelength of 1075.5 nm. These parameters were found to give an optimum coherent pulse break-up into a FWM cascade for a fully coherent seed [11]. For each set of parameters 500 simulations were carried out, except for cases with a higher peak power or numerical resolution where only 250 simulations were used, which was found to be sufficient to get consistent statistical results. Loss was neglected and care was taken to avoid time-wrapping and conserve the photon number.

The coherence of the seed relative to the pump is quantified by the two-frequency cross-spectral density (CSD) function [17],

$$|\text{CSD}(\omega_i, \omega_j)| = \left| \frac{\langle \tilde{A}^*(\omega_i) \tilde{A}(\omega_j) \rangle}{\sqrt{\langle |\tilde{A}(\omega_i)|^2 \rangle \langle |\tilde{A}(\omega_j)|^2 \rangle}} \right|, \quad (4)$$

which characterises the correlation between frequencies of the SC spectrum. In contrast, the spectral coherence function measures the correlation between an ensemble of SC spectra at

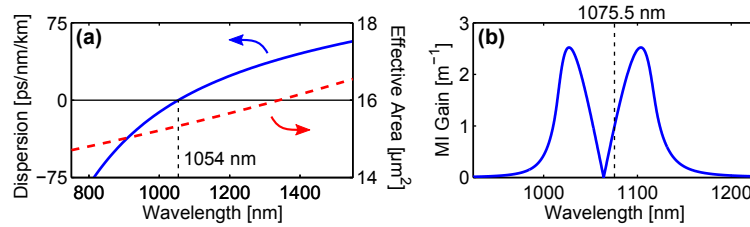


Fig. 1. (a) Dispersion and effective area for the used PCF with pitch $\Lambda = 3.6 \mu\text{m}$ and hole-to-pitch ratio $d/\Lambda = 0.52$. (b) MI gain as a function of wavelength for the 1064 nm pump with a peak power of 250 W. The dashed line marks the seed wavelength.

a single frequency. Figure 2 shows the ensemble averaged input spectra and CSD function for varying seed linewidth; the CSD function is calculated relative to the pump (1064 nm) and shows how the seed becomes increasingly incoherent with the pump when the linewidth is increased. The seed is partially coherent with the pump for linewidths larger than 1 GHz. The Lorentzian shape of the phase-diffusion model applied to the seed is clearly visible in the spectra, and it is seen that the seed linewidth is a simple way of changing the coherence of the seed relative to the pump.

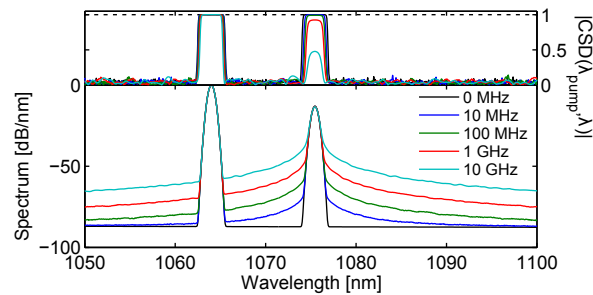


Fig. 2. Ensemble averaged input spectra (bottom) and cross-spectral density (CSD) function relative to the pump (top) for varying seed linewidth, $\Delta\nu_{\text{FWHM}}$.

In [14] it was suggested to reshape the Lorentzian power spectrum into a Gaussian, which falls off much more rapidly. A Gaussian noise spectrum was demonstrated to give good agreement between simulations and experiments. This approach can, however, not be used for the seed linewidths considered in this work, as we shall elaborate on in more detail in the next section.

3. Results

The results of seeding with varying seed linewidth is shown in Fig. 3 for a select number of linewidths. In the absence of a seed the spectral broadening is initiated by noise-induced MI, as seen in Fig. 3(a). Unseeded MI amplifies a single set of side-bands that eventually evolves into solitons and dispersive waves. This results in an incoherent spectrum with unity SNR, except near the residual pump. By introducing a coherent seed near the pump, the spectral broadening is initiated by the coherent amplification of a cascaded FWM comb, as seen in Fig. 3(b). Subsequently, the comb leads to soliton formation. The resulting spectrum is coherent and with high SNR over most of the spectral bandwidth, where there is MI gain to allow a coherent broadening. When the linewidth of the seed is increased, as seen in Figs. 3(c)-(f), the

broadening is still initiated by a FWM cascade, but the contrast of the comb is gradually washed out. This leads to a significant reduction of the coherence and SNR of the generated spectrum. In fact, for a seed linewidth in the GHz range, the noise properties are only marginally better than for an unseeded SC.

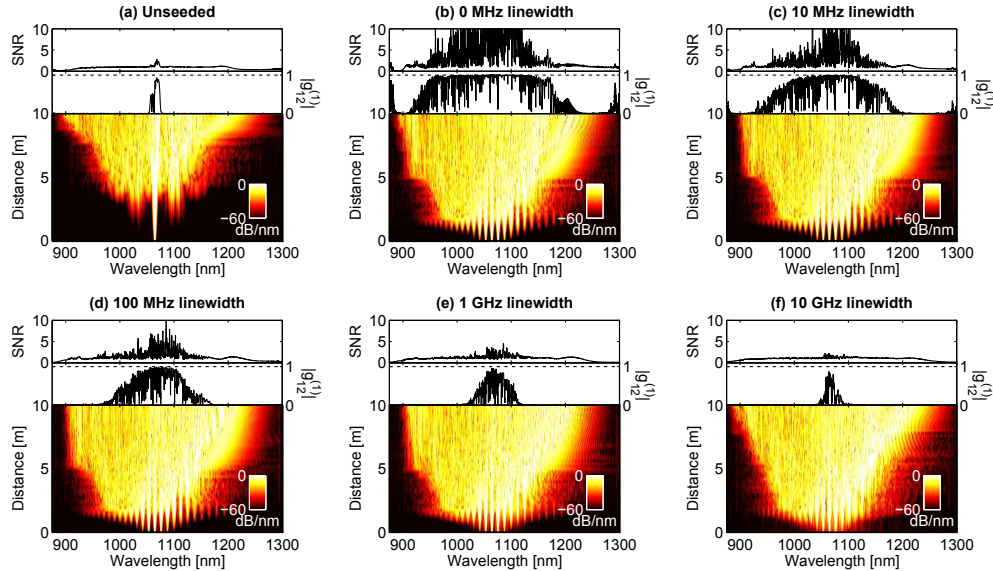


Fig. 3. Single shot simulations of (a) unseeded and (b)-(f) seeded SC generation with varying seed linewidth, $\Delta\nu_{\text{FWHM}}$. The top rows show the ensemble calculated spectral coherence function and SNR at the fiber output (10 m).

To further illustrate the effect of seeding with a noisy seed, we show in Fig. 4 the ensemble calculated spectrum, spectral coherence function and SNR at a propagation distance of 1 m for the same seed linewidths used in Fig. 3. The input spectrum from a single shot is shown by a grey line. The comb structure is clearly visible in all cases, except the unseeded where only a single set of side-bands is incoherently amplified. In Fig. 4(c) the comb structure and noise properties are similar to those of the fully coherent seed in Fig. 4(b). However, when the seed linewidth is increased in Figs. 4(d)-(f) the fringe contrast of the comb is decreased and the coherence and SNR significantly diminished.

Figures 2 and 4 show how the Lorentzian noise spectrum raises the noise floor above that of the one photon per mode background noise. To confirm that the noise properties of the generated SC are indeed controlled by the phase noise of the seed and not the higher background noise imposed by the Lorentzian spectrum, we performed additional simulations with a background of multiple photons per mode and a fully coherent seed. To this end, we show in Fig. 5(a) a comparison of the ensemble calculated spectra, coherence and SNR for a coherent seed with normal (black line) and raised (blue line) background noise for which the noise floor at the pump is at approximately -90 and -70 dB/nm, respectively. The noise floor of -70 dB/nm corresponds to the average noise level at the pump from a partially coherent seed with a 1 GHz noise linewidth (see Fig. 2). It is seen that the outermost fringes of the comb are not generated when they are below the noise background. More importantly, we find that the comb is always generated with high fringe contrast, SNR and coherence irrespectively of the background noise level when the seed is fully coherent. In contrast, Fig. 5(b) shows a comparison of the results obtained for seed linewidths of 0 MHz and 1 GHz (average noise at the pump equal to -70 dB/nm) with a normal

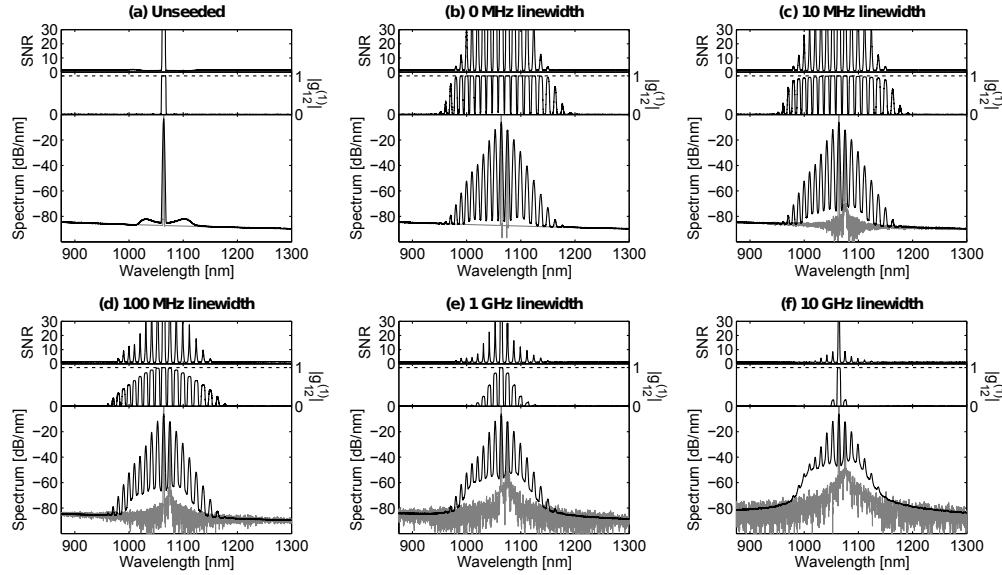


Fig. 4. Ensemble calculated spectra, coherence and SNR at a propagation distance of 1 m for (a) unseeded and (b)-(f) seeded SC generation with varying seed linewidth, $\Delta\nu_{FWHM}$. The grey spectra show single shot input.

one photon per mode noise background, corresponding to Figs. 4(a) and 4(e). When the noise linewidth of the seed is increased, the fringe visibility of the comb is now seen to degrade much more severely and only the central fringe is generated with full coherence and high SNR. This is in sharp contrast to the effects of increasing the noise background, which leads us to conclude that the phase noise of the seed - and not the higher background noise level - is indeed the dominant effect responsible for the SC noise properties seen in Figs. 3-4.

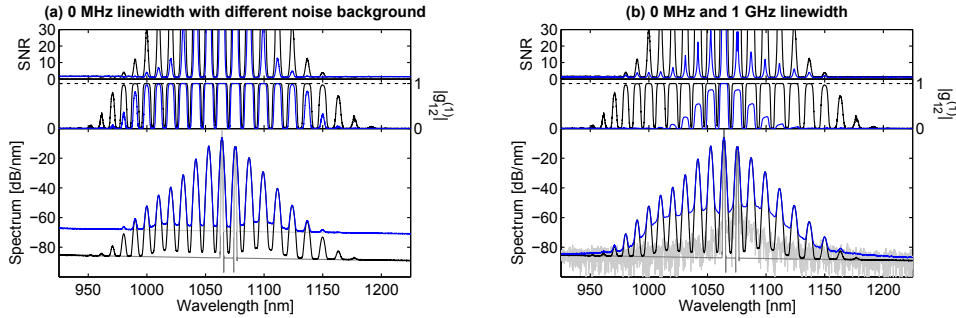


Fig. 5. Comparison of ensemble calculated spectra, coherence and SNR at a propagation distance of 1 m for (a) coherent seeding with normal (black) and raised (blue) background noise levels, and (b) seed linewidths of 0 MHz (black) and 1 GHz (blue) with a normal noise background. The grey spectra show single shot input.

The results are summarised in Fig. 6 by the overall coherence as a function of seed linewidth. We show the results of seeding for pump peak powers of 125, 250 and 500 W, respectively. The peak power of the seed was in all cases 5% of the pump. For the highest peak power only 250 simulations were carried out. As a further investigation, we also checked the results for a CW

seed. The CW field was approximated by a 10th order super-Gaussian with a $1/e$ width of 15 ps and a peak power of 1% of the pump, which gives a field that is constant seen by the pump pulse. In all cases, Fig. 6 clearly shows a decrease in the overall coherence with increasing seed linewidth. For the pulsed seed there is a major decrease in the overall coherence with increasing peak power. This is due to the increasingly turbulent dynamics caused by a higher number of solitons and spectra exceeding the MI gain bandwidth [11]: the spectral evolution after the pulse break-up is dominated by highly amplitude and phase-sensitive soliton collisions that significantly degrade the coherence. When the soliton number is increased there will be a corresponding increase in the number of such collisions and hence a decrease in the coherence of the generated spectrum. The seed linewidth at which the coherence is decreased by 25% relative to that of the coherent seed is marked with a black star. It is seen that the tolerance to phase noise on the seed is significantly decreased with increasing pump peak power, which again can be explained as a consequence of the increased number of solitons and collisions: when the number of collisions increases there will be a higher sensitivity to the initial shape and phase of the solitons, and hence to the phase noise of the seed that is responsible for the pulse break-up and soliton formation. For all peak powers there is however a clear decrease in overall coherence when the seed linewidth is increased above the MHz level. The same tendency is observed for the CW seed, which highlights the generality of the results: the phase noise of the seed must be weak in order for the pulse break-up and generated SC to be coherent.

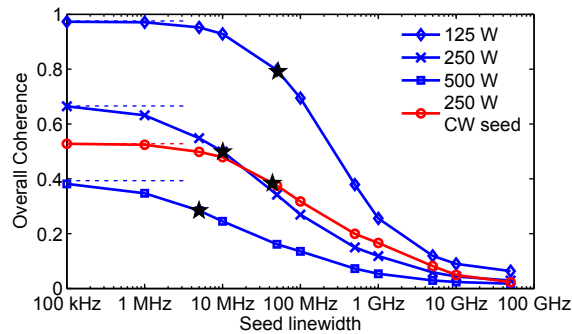


Fig. 6. Overall coherence as a function of seed linewidth, $\Delta\nu_{FWHM}$, for pulsed and CW seeds at the fiber output (10 m). For the pulsed seed is shown results of pump peak powers of 125, 250 and 500 W, respectively. The pulsed seeds had 5% of the peak power of the pump and the CW seed had 1%. The horizontal dashed lines mark the overall coherence for a fully coherent seed and the black stars mark the seed linewidth at which the coherence is decreased by 25%.

The results presented so far were all calculated using a numerical resolution of 19.1 GHz, which is insufficient to resolve most of the relevant seed linewidths. To illustrate the implications of this, we show in Fig. 7(a) the overall coherence as a function of seed linewidth for various numerical frequency resolutions from 76.3 to 2.38 GHz and a peak power of 125 W. The frequency resolution was changed by fixing the temporal resolution and increasing the number of discretisation points from 2^{12} to 2^{17} , everything else was kept constant. For resolutions higher than 4.77 GHz (2^{16} points) only 250 simulations were carried out. The overall coherence is clearly observed to decrease with increasing frequency resolution. This tendency is even clearer in Fig. 7(b), where the overall coherence is shown as a function of frequency resolution down to 0.596 GHz (2^{19} points) for four fixed seed linewidths of 0.01, 0.1, 1 and 10 GHz, respectively. It is seen that the overall coherence converges when the frequency res-

olution approaches the seed linewidth, as expected. The 10 and 100 MHz seed linewidths can not be resolved and hence do not converge. Frequency resolutions smaller than ~ 1 GHz, which generally requires more than 2^{17} discretisation points, are computationally very intensive to simulate and it is therefore not possible to resolve noise linewidths much finer than 1 GHz. This also explains why it is not possible to use the Gaussian shaped noise model suggested in [14]: a Gaussian with a linewidth in the MHz is too narrow to be resolved numerically, whereas a long-tailed Lorentzian spectrum falls off sufficiently slowly to be at least partially resolved.

We emphasize that the results presented in this paper are all *qualitatively* valid: when the seed linewidth is increased, the seed becomes increasingly incoherent with the pump as shown in Fig. 2. This results in an incoherent pulse break-up and correspondingly noisy and incoherent SC as seen in Figs. 3-4. These results clearly highlight the need for seeding with a seed that is at least partially coherent with the pump. However, one must be careful with making quantitative conclusions about noise and coherence based on the phase-diffusion model, unless the numerical resolution is at least comparable to the noise linewidth.

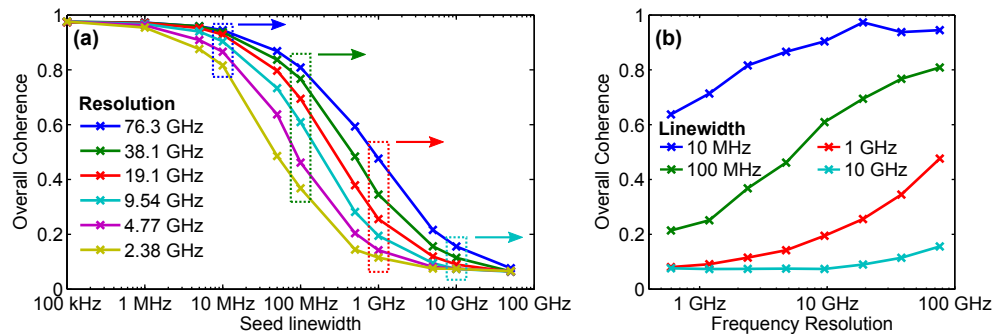


Fig. 7. (a) Overall coherence as a function of seed linewidth, $\Delta\nu_{\text{FWHM}}$, for varying numerical frequency resolution. (b) Overall coherence as a function of numerical frequency resolution for the four seed linewidths marked by dotted boxes in (a). In all cases the pump peak power was 125 W.

The decrease in overall coherence with increasing numerical resolution shows that the maximum tolerable phase-noise of the seed is in fact quite small, although we can not accurately determine a quantitative value. Interestingly, Figs. 3-4 shows that the noise properties of the generated SC presented are deteriorated even when the linewidth of the seed is in the MHz range, although the seed is still coherent with the pump at the input ($\text{CSD}(\lambda_{\text{pump}}, \lambda_{\text{seed}}) \approx 1$) as seen in Fig. 2. A linewidth of 100 MHz corresponds to just 0.4 pm, and since the actual tolerable seed linewidth will be smaller, this again clearly highlights the need for seeding coherently to achieve a coherent SC. Importantly, these results dictate which mechanisms can be used to generate the seed. It would be highly desirable to generate the seed by some frequency-shifting technique of the pump in an all-fiber design. A simple approach would be to use the Raman Stokes line as a seed. Unfortunately, a Raman amplified seed will generally not be coherent and have a significant noise linewidth. This exact approach was tested in [18], where no noise improvement was observed. However, a high peak power was used, which will by itself lead to noisy spectra due to chaotic solitonic dynamics irrespectively of the seed [11].

Finally, we would like to point out that FWM is a parametric and hence phase sensitive process. It was therefore to be expected that the amplification of a FWM comb eventually becomes noisy when the phase noise of the seed is increased. In the context of SC generation, the results presented in this work are nonetheless important, as they show just how sensitive

the seeding process is to the phase noise of the seed. In this paper we have only investigated the influence of phase noise on the seed for a single set of parameters of the pump and seed. In [11] it was found that seeding (under reasonable conditions) leads to the amplification of a number of FWM side-bands, and that the best noise improvement occurs for small pump-seed frequency offsets where a large number of FWM side-bands is coherently amplified. We have thus chosen the optimum seeding conditions as the starting point for this work. Seeding relies on the coherent amplification of FWM side-bands, which, as we have shown here, requires a seed that is at least partially coherent with the pump. Since FWM is a parametric process, we hence expect the results presented in this article to be valid for a wide range of parameters. A complete analysis of the exact dependence on, e.g., seed wavelength and power is beyond the scope of this manuscript.

4. Conclusions

In conclusion, we investigated the influence of the phase coherence of the seed on seeded SC generation. Numerical simulations were performed, in which the phase noise of the seed was modelled by a physically justified phase-diffusion model. For a coherent seed placed at the optimum near the pump, the pulse break-up is caused by a coherent amplification of a frequency comb through FWM. When phase noise is added to the seed, the pulse break-up and generated SC eventually become noisy. It was found that a coherent pulse break-up requires a nearly phase coherent seed, which limits the mechanisms that can be used to generate the seed. These tendencies were observed both for pulsed and CW seeding.

Acknowledgments

We thank the Danish Agency for Science, Technology and Innovation for financial support.